Inorganic Chemistry

ARTICLE

pubs.acs.org/IC

Liquefaction of Solid-State BH_3NH_3 by Gaseous NH_3

Liang Gao,[†,§] Haocheng Fang,[‡,§] Zhenhua Li,[‡] Xuebin Yu,[*,†] and Kangnian Fan[‡]

[†]Department of Materials Science, Fudan University, No. 220 Handan Road, Shanghai, 200433, P.R. China

[‡]Shanghai Key Laboratory of Molecular Catalysis & Innovative Materials, Department of Chemistry, Center for Theoretical Chemical Physics, Fudan University, No. 220 Handan Road, Shanghai, 200433, P.R. China

Supporting Information

ABSTRACT: This paper reports for the first time that under ammonia atmosphere, ammonia borane (AB) reversibly absorbs up to at least 6 equiv of NH_3, forming liquid $AB(NH_3)_n$ ($n = 1-6$) complexes at 0 °C. Reasonable structures for $AB(NH_3)_n$ were identified via density functional theory calculations, which indicate that the strong classical hydrogen bond formed between the lone pair of NH_3 and the -NH_3 of AB is the driving force for the absorption of ammonia by AB. By use of the van't Hoff equation, the enthalpy change (ΔH) for AB to absorb one NH_3 was determined to be −2.24 kcal/mol, which is in good agreement with the theoretical calculations. Other organic amines were screened to further confirm the role of the N lone pair; only 1,4-diazabicyclo[2.2.2]octane (DABCO) formed a stable adduct, which X-ray structural analysis showed was the DABCO-BH_3 species. Finally, Raman spectra of $AB(NH_3)_n$ were collected, and its unique spectral features are also discussed.

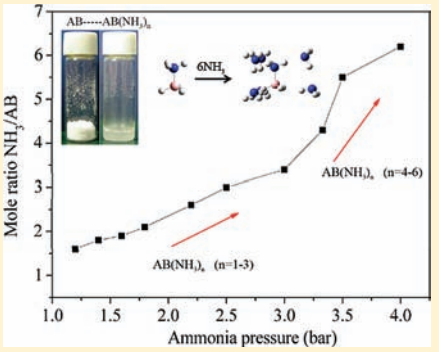

INTRODUCTION

There has been much work for more than 60 years on amine boranes, among which, ammonia-borane (AB) has received disproportionately more attention than any other Lewis acid/base adduct of this type for a long time.[1] AB was first successfully prepared from diammoniate of diborane (DADB) in 1955 by Shore and Parry.[2] Besides its promising nature for hydrogen storage (high H-capacity and favorable kinetics),[3−6] long-term fundamental research on AB has also had impact on our understanding of basic chemistry, in such aspects as unconventional hydrogen bonds: dihydrogen bonds;[7−9] a typical mode for double H-transfer because of its significant polarization;[10,11] and B−N polymer synthesis.[12] In 1947, Burg proposed the empirical equilibrium $NH_4(BH_3)_2NH_2 + 2xNH_3 \leftrightarrow 2(BH_3NH_3)\text{-}2xNH_3$,[13] implying an essential correlation between $NH_4(BH_3)_2NH_2$ and BH_3NH_3. However, there is no convincing evidence provided in that paper to favor such equilibrium. On the other hand, the subsequent isolation of BH_3NH_3 shows definitely that it does not exist in labile equilibrium with the "diammoniate", so the postulated equilibrium is untenable.[2,14] Since then, a series of chemical experiments have resolved the ambiguity in favor of the now-accepted borohydride.[15−19] It is noteworthy that most of these experiments were run in liquid ammonia solution; however, there is no detailed research regarding the interaction of AB and gaseous NH_3. More interestingly, ammonia displacement of the borane-tetrahydrofuran (THF) complex is one of the original syntheses of AB, but since the ammonia was distilled away, the authors failed to observe the appearance of $(BH_3NH_3)\text{-}xNH_3$.[14] Given the history of B−N complex investigation and current intensive interest in AB, it is clear that the interaction between AB and NH_3 is of high value and worth researching more deeply.

In addition, BH_3NH_3 complexes of methane, hydrogen cyanide, ammonia, water, methanol, and hydrogen fluoride have been widely investigated and compared as typical models of dihydrogen bond and polarity description using theoretical calculations.[20−23] Many such studies have focused on the unconventional hydrogen bonds of AB and its derivatives.[8,24−30] Their properties and mechanisms of hydrogen storage are also attractive to researchers.[31−33] Li[25] and Meng et al.[20] calculated a series of complexes characterized by N−H···H−B bonds, including $ABNH_3$.

Herein, we report an experimental phenomenon, that is, under 1−4 bar ammonia, AB reversibly absorbs up to 6 equiv of NH_3 and becomes liquid at 0 °C.[34] This is the first experimental description of the formation of $AB(NH_3)_n$ complexes. Reasonable structures for $AB(NH_3)_n$ complexes were identified via density functional theory (DFT) calculations and compared well with the results of different experiments.

EXPERIMENTAL AND THEORETICAL METHODS

Apparatus. During X-ray diffraction (XRD) measurements, samples were mounted in a glovebox, and amorphous polymer tape was used to cover the surface of the powder to avoid oxidation. During infrared (IR) measurements (using KBr pellets), samples were loaded into a closed tube with CaF_2 windows. Raman spectra were collected at room temperature in backscattering geometry using the 632.8 nm line of an

Received: November 6, 2010
Published: April 14, 2011

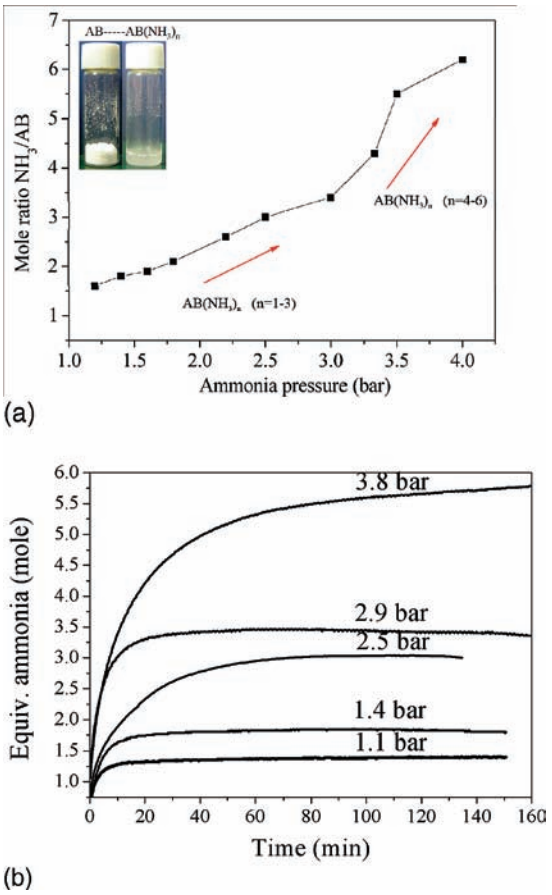

Figure 1. (a) Accumulated NH_3 capacity absorbed by AB increases along with increasing ammonia pressure. The inset photograph shows AB and the liquid-state ammonia adduct of AB. (The line is merely a guide to the eye.) (b) AB-ammonia absorption curves at various pressures.

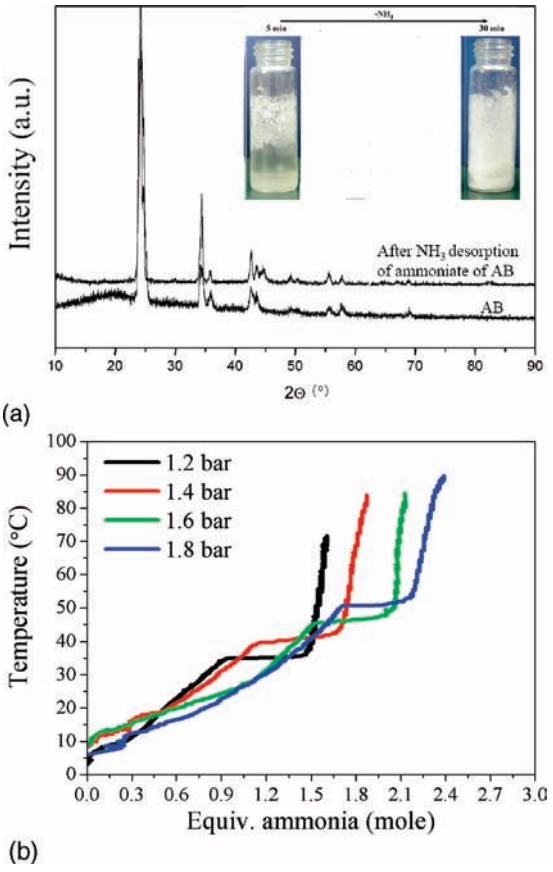

Figure 2. (a) XRD patterns of pristine AB and the ammoniate of AB after ammonia desorption. (b) TPD curves of ammonia released from ammoniate of AB under various ammonia pressures. Inset photographs in (a): on 30 min exposure to air, the ammonia is totally released from the $AB(NH_3)_n$ complexes, and a white powder is formed, which is confirmed by XRD to be pure AB.

Ar+-ion gas laser with a power of 100 mW, and the samples were mounted with a thin cover glass to isolate them from air.

The experimental details for the ammonia absorption, including setup and measurement method description, are shown in Supporting Information, Figure S1.

Samples. Ammonia borane (AB, 97.0%), pyridine (pyr., 99.9%), bipyrdine (bipyr., 99.0%), 1,4-diazobicyclo(2,2,2) octane (DABCO, 99.0%), and triethylamine $(Et)_3N$, 99.0%) were purchased from Sigma Aldrich and used directly. Tetrahydrofuran (THF) was dried by sodium reflux. Ammonia (99.99% Sinopharm Chemical Reagent Co. Ltd.) was dried using soda-lime.

Theoretical Methods. Quantum chemical calculations were performed to predict the structures and vibrational frequencies of the observed reaction products using the Gaussian 09 package. The double hybrid density functional mPW2PLYP, recently proposed by Grimme et al.,[35] was used. This functional uses Kohn−Sham unoccupied orbitals to calculate MP2-type correlation energy and is reported to be quite reliable.[36,37] Augmented correlation-consistent double- or triple-ζ valence basis sets (aug-cc-pVXZ, X = D and T)[38] were used for hydrogen, boron, and nitrogen. Unless otherwise noted, in all the calculations, geometry optimizations and frequency calculations were carried out in the aug-cc-pVDZ basis set. Single-point energy calculations on the geometry optimized for the aug-cc-pVDZ basis set were performed in the aug-cc-pVTZ basis set to give accurate energetic results. Test calculations on the AB molecule indicate that the mPW2PLYP functional is quite reliable for the system studied here. As shown in the Supporting Information, Table S1, the theoretical bond lengths of the B−N, B−H, and N−H bonds agree well with the microwave spectroscopy results.

To account for the solvent effect (ammonia for this work), the calculations on the solution were performed using the integral equation formalism of the polarizable continuum model (IEFPCM),[39] with the radii and nonelectrostatic terms based on Truhlar and co-workers' solute electron density (SMD) solvation model.[40] The static dielectric constant and the optical dielectric constant for pure ammonia that were used in the polarizable continuum model (PCM) calculations are 22.0 and 2.0, respectively.[41] For all the PCM calculations, only single-point energy calculations were performed on the geometry optimized in the gas phase.

RESULTS AND DISCUSSION

As shown in Figure 1, the accumulated NH_3 absorption capacity of AB increases with increasing ammonia pressure. Two stages can be clearly observed in Figure 1a. Along with increasing of n in $AB(NH_3)_n$, the derivative of mole ratio on the ammonia pressure increases suddenly on the plot of NH_3/AB mole ratio vs ammonia pressure in the range of n = 3∼4. This remarkable turning point most likely implies that there are two types of binding modes in $AB(NH_3)_n$ complex, consistent with our optimization structure results (vide infra). Therefore, it may be deduced that there are two different absorption mechanisms

dx.doi.org/10.1021/ic200373g |Inorg. Chem. 2011, 50, 4301–4306

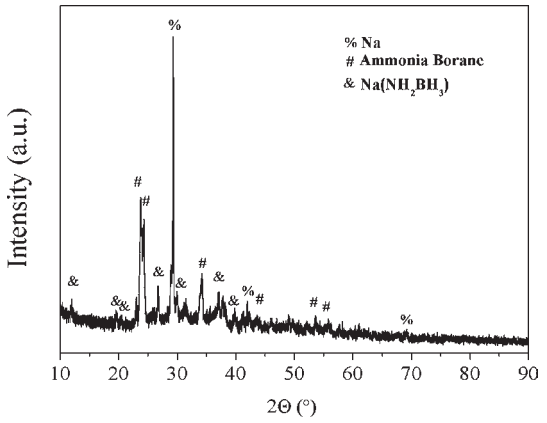

Figure 3. X-ray diffraction pattern of the reaction product after mixing Na and AB-NH_3 complex under 3 bar ammonia at 0 °C. Peak locations for Na, and BH_3NH_3 were obtained from #22−0948, and #13−0292. Peak locations for $Na(NH_2BH_3)$ were obtained from ref 45.

or two kinds of $AB(NH_3)_n$ structures involved in the process of ammonia absorption. As shown in the inset photograph, $AB(NH_3)_n$ becomes liquid at room temperature. This result could be attributed to complex competition between AB-AB and AB-NH_3 by different interactions, such as with dipoles, hydrogen bonds, and dihydrogen bonds.

Ammonia desorption can be confirmed by temperature programmed desorption (TPD) curves as well as by the XRD patterns after the NH_3 is evaporated off $AB(NH_3)_n$, as shown in Figure 2. Note that the liquid ammoniate of AB is not stable at room temperature in air and the ammonia breaks away from AB within 30 min (inset photograph of Figure 2(a)), so it is hard to confirm the mole ratio of NH_3/AB by using the conventional characterization method. It is noteworthy that the prospect of $AB(NH_3)_n$ combining chemically to form a liquid state is promising as a novel technique of confining AB by using nanoscaffold loading, which is a key technology facilitating hydrogen release from AB.[42,43]

The chemical structure of DADB was controversial for a long time, before a series of chemical experiments resolved the ambiguity in favor of the now-accepted borohydride by the reaction of an alkali metal.[44] To clarify whether a similar chemical species to DADB appears in the $AB(NH_3)_n$ complexes, the reaction of sodium with the liquid $AB(NH_3)_n$ complexes was examined, and identification of the reaction products was attempted. On the other hand, AB was reported to be soluble in liquid ammonia,[14] so another interesting question is how concentrated liquid NH_3 solutions of AB prepared many years ago compare to the NH_3 complexes described here. This may be clarified by comparing their reaction products. XRD patterns of the products under 3 bar ammonia at 0 °C are shown in Figure 3. There are bare patterns assigned to $NaBH_4$ patterns according to PDF card (#09-0386). This suggests that the BH_4^- anion is unlikely to be one of the chemical species featured in the $AB(NH_3)_n$ complexes. The major solid-phase residue is Na and ammonia borane. Interestingly, liquid AB-NH_3 reacts with excess Na to yield the recently described salt $Na(NH_2BH_3)$ as a product, which is similar to the reaction occurring in THF solution.[45,46]

To identify the structures of the $AB(NH_3)_n$ complexes and clarify the driving force for $AB(NH_3)_n$ formation, geometry optimization and natural bond orbital (NBO) analysis were performed, using the mPW2PLYP method. Nine possible $AB(NH_3)_n$

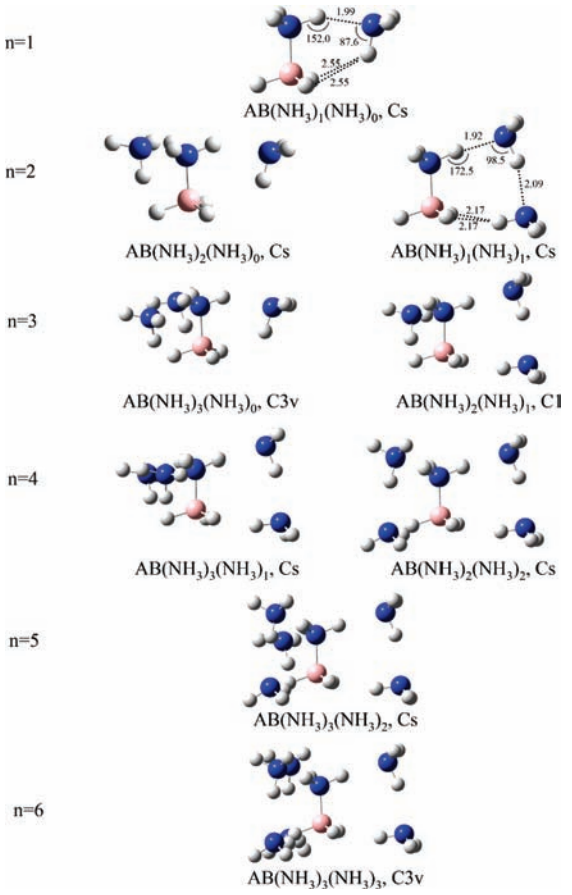

Figure 4. Low-energy structures of the $AB(NH_3)_n$ complexes. The complexes are named $AB(NH_3)_x(NH_3)_y$, where x represents the number of ammonias forming classic hydrogen bonds with NH_3 of AB (α site) while y represents the number of ammonias forming dihydrogen bonds with BH_3 of AB (β site). Some of the bond lengths (in Å) and angles (in degrees) are specified. The blue, pink, and white balls represent the nitrogen, boron, and hydrogen atoms, respectively. Point groups of these complexes are also given.

($n = 1-6$) complexes have been optimized, and they are shown in Figure 4.

In $AB(NH_3)_n$ ($n = 1-6$), there are two types of hydrogen bond between ammonia and AB. One is the classic hydrogen bond formed between NH_3 of AB (identified as the α site) and ammonia, and the other is the so-called dihydrogen bond formed between BH_3 of AB (identified as the β site) and ammonia. Therefore, $AB(NH_3)_n$ ($n = 1-6$) can be rewritten as $AB(NH_3)_x(NH_3)_y$ ($x = 1-3, y = 0-3$), where x and y represent the number of α and β site ammonias, respectively. For $AB(NH_3)_1$, only the $AB(NH_3)_1(NH_3)_0$ complex can be optimized, because the classic hydrogen bond is stronger than the dihydrogen bond. $AB(NH_3)_2$ can be viewed as adding one NH_3 to $AB(NH_3)_1$. Unlike $AB(NH_3)_1$ the second NH_3 can attach at either the α site or the β site, forming either $AB(NH_3)_2(NH_3)_0$ or $AB(NH_3)_1(NH_3)_1$, with the former complex more stable than the latter. This is because although the dihydrogen bond is weaker than the classic hydrogen bond, the second NH_3 in $AB(NH_3)_1(NH_3)_1$ can form not only a dihydrogen bond with the BH_3 group, but also a classic hydrogen bond with the first NH_3 on the α site. For $AB(NH_3)_3$, only $AB(NH_3)_2(NH_3)_1$ and $AB(NH_3)_3(NH_3)_0$ can be optimized, but not the $AB(NH_3)_1(NH_3)_2$ and

dx.doi.org/10.1021/ic200373g |Inorg. Chem. 2011, 50, 4301–4306

Table 1. Average Binding Energies (E_b) in kcal/mol of AB-$(NH_3)_n$ and the Binding Energies of $(NH_3)_2$ and $(AB)_2$ at 0 K in Ammonia Solution[a]

	E_b
$AB(NH_3)_1(NH_3)_0$	−2.50
$AB(NH_3)_2(NH_3)_0$	−2.19
$AB(NH_3)_1(NH_3)_1$	−1.97
$AB(NH_3)_3(NH_3)_0$	−1.91
$AB(NH_3)_2(NH_3)_1$	−1.91
$AB(NH_3)_3(NH_3)_1$	−1.81
$AB(NH_3)_2(NH_3)_2$	−1.82
$AB(NH_3)_3(NH_3)_2$	−1.80
$AB(NH_3)_3(NH_3)_3$	−1.81
$(NH_3)_2$	−0.87
$(AB)_2$	−1.46

[a] All energies are corrected by the zero point energies. Average binding energies of $AB(NH_3)_n$ are defined by $E_b = ((1)/(n))(E^0_{AB(NH_3)n} - nE^0_{NH_3} - E^0_{AB})$.

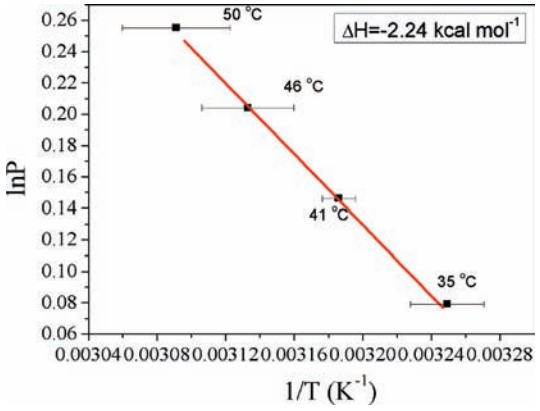

Figure 5. Van't Hoff profile of the $AB(NH_3)_n$ complexes.

$AB(NH_3)_0(NH_3)_3$ complexes, because for one NH_3 to occupy the β site, there must be one unused NH_3 on the α site with which to form a classic hydrogen bond. Therefore, in the $AB(NH_3)_x(NH_3)_y$ complexes, y must be less or equal to x, and only nine possible structures of $AB(NH_3)_n$ can be optimized.

Calculated binding energies strongly support the experiments. Table 1 lists the average binding energies (E_b) of $AB(NH_3)_n$ (n = 1−6), and the binding energies of $(NH_3)_2$ and $(AB)_2$. Average binding energies of $AB(NH_3)_n$ at 0 K are defined by $E_b = ((1)/(n))(E^0_{AB(NH_3)n} - nE^0_{NH_3} - E^0_{AB})$, where $E^0_{AB(NH_3)n}$, $E^0_{NH_3}$, and E^0_{AB} are the energies of $AB(NH_3)_n$, NH_3, and AB, respectively, at 0 K in solution. For the $AB(NH_3)_n$ (n = 1−6) complexes, the average binding energies obtained range from −2.50 to −1.80 kcal/mol. As the number of ammonia increases, the binding energies become less negative when $n \leq 3$ and change little when $n > 3$. This perhaps can explain why there is a change of slope in the plot shown in Figure 1a, which implies that there are two different absorption mechanisms, acting before and after approximately n = 3. For the reaction $AB(s) + nNH_3(g) \rightarrow AB(NH_3)_n(l)$, the change in enthalpy per mole of NH_3 (ΔH) can be calculated from the equation $\Delta H = E_b - RT$. The resulting ΔH at 40 °C ranges from −3.10 to −2.43 kcal/mol. As shown in Figure 5, the corresponding experimental value over the temperature range between 35 and 50 °C is determined to be −2.24 kcal/mol, according to the van't Hoff equation. The good agreement between experimental and theoretical results on ΔH is strong support for the reliability of the theoretical calculations on the structure and energetics of the $AB(NH_3)_n$ complexes.

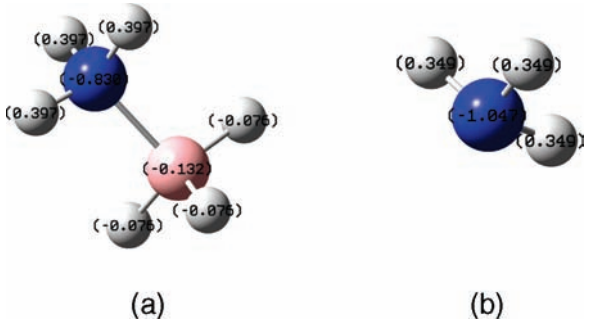

Figure 6. NBO charge distribution of AB and NH_3. The blue, pink, and white balls refer to the nitrogen, boron, and hydrogen atoms, respectively.

As mentioned above, both the classic hydrogen bond and the dihydrogen bond play important roles in forming the $AB(NH_3)_n$ complexes. Comparing the binding energies of $(NH_3)_2$ and $(AB)_2$, as listed in Table 1, with those of the $AB(NH_3)_n$ complexes, it can be seen that the dihydrogen bond between two AB is weaker than the classic hydrogen bond between AB and NH_3, but is stronger than the classic hydrogen bond between two NH_3. The binding energy between AB in the solid is hard to calculate, since the current available quantum software codes cannot perform periodic calculations using the mPW2PLYP functional, while the performance of other functionals implemented in periodic quantum software codes is very bad on weak interactions. Alternatively, the binding energy of AB in the solid is estimated by the following procedure: (1) Cut nine AB molecules from the solid geometry, where one AB is surrounded by eight AB molecules, and calculate the energy of the cluster. (2) Take the center AB molecule out and calculate the energy of the remaining eight AB molecules. (3) Calculate the energy change. The binding energy calculated is −1.33 kcal/mol, very close to the −1.36 kcal/mol between two AB molecules in solution. Therefore, the calculation results indicate that the binding between AB molecules in a solid is weaker than between AB and ammonia. This is the reason why AB can absorb ammonia. In addition, once AB is surrounded by NH_3, that is, forming the $AB(NH_3)_n$ complexes, the interaction between $AB(NH_3)_n$ is greatly weakened. In the extreme case where n = 6, the lone pairs of NH_3 in $AB(NH_3)_6$ have all been used, and $AB(NH_3)_6$ can no longer form either classic hydrogen bonds or dihydrogen bonds with each other. This can explain why solid AB becomes liquid after absorbing NH_3.

To understand the interaction between AB and ammonia, NBO[47,48] charge analysis has been performed on AB and NH_3. As shown in Figure 6, the hydrogen atoms on the NH_3 of AB have a collective charge of +0.397e, while the hydrogen atoms of the ammonia molecule have +0.349e. The reason for the more positively charged H atoms on NH_3 of AB is the donation of the lone pair electrons on N atoms to B atoms in forming AB, while N, in turn, pulls more electrons from H. This explains why NH_3 binds more strongly with AB than with itself.

To further confirm the role of the lone pair electrons of N in AB in forming hydrogen bonded complexes, a series of

dx.doi.org/10.1021/ic200373g |Inorg. Chem. 2011, 50, 4301–4306

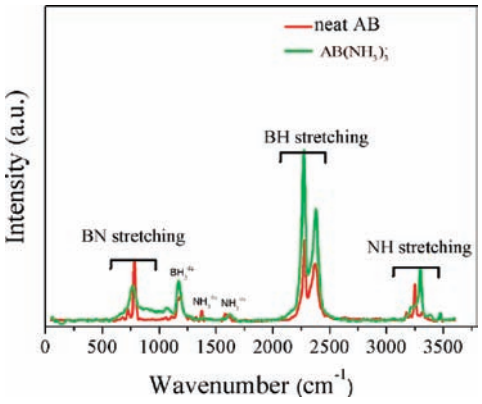

Figure 7. Raman spectra of AB and $AB(NH_3)_3$ (in cm^{-1}).

organic amines, including pyridine (pyr.), bipyrdine (bipyr.), 1,4-diazobicyclo(2,2,2) octane (DABCO), and triethylamine $(Et)_3N$, were selected to react with AB to reveal whether some stable products could be obtained. However, only the addition of DABCO to AB, followed by extraction and crystallization from THF solution, is able to yield a novel product and form a suitable crystal for XRD (Supporting Information, Figure S2−S5). It seems that the steric hindering effect plays the primary role in the reaction between AB and DABCO: the $-NH_3$ group is completely displaced by DABCO from AB (Supporting Information, Figure S6). This reaction, in turn, implies the novelty and particularity of the formation of $AB(NH_3)_n$ complexes.On the other hand, it is of interest to study the interaction between NH_3 and another NH_xBH_x compounds, for example, NH_4BH_4, whose structure was well determined by Flacau et al.[49] The refined structure and Raman spectroscopy of NH_4BH_4 safely confirms the presence of NH_4^+ and BH_4^- ions. Comparing with NH_3 of AB, NH_4^+ of NH_4BH_4 may possess more positively charged H atoms, which are more favorable to attract the lone pairs of NH_3 to form $NH_4BH_4(NH_3)_n$ via the classical hydrogen bond: H_4BNH_3 —H←:NH_3.

Raman spectroscopy was also employed to study the bonds in AB and liquid $AB(NH_3)_n$ complexes, since (1) it is easy to sustain a particular ammonia pressure by sealing $AB(NH_3)_n$ in a glass chamber during Raman measurement; and (2) the B−N bond can be identified clearly in Raman spectra. Raman spectroscopy of AB and of the ammoniate of AB with sufficient ammonia absorbed (4 bar, 0 °C) was conducted. Since these two spectra show few differences, no new chemical group can be identified in the Raman spectra. All of these experimental data show great correspondence with the results from our calculations using the $AB(NH_3)_3$ model that we have proposed (Supporting Information, Figure S7).[50] $AB(NH_3)_3$ was selected because $AB(NH_3)_n$ complexes are very similar to each other and $AB(NH_3)_3$ has the same point group C_{3v} as saturated $AB(NH_3)_6$, so that it is much simpler to perform the Raman frequency calculations.

As shown in Figure 7, for the neat solid AB, the 724 and 784 cm^{-1} peaks can be assigned to B−N stretching vibrations. The higher frequency peak is due to the symmetric stretching of the B−N bonds, while the lower one is due to antisymmetric stretching of the B−N bonds. The vibrational frequencies corresponding to the symmetric and antisymmetric B−H stretching are located at 2277 and 2374 cm^{-1}, respectively, locations which are in good agreement with the theoretical values of 2401 and 2374 cm^{-1} for $(AB)_2$. The 3249 and 3490 cm^{-1} peaks are assigned to N−H stretching. All the main vibrational frequencies are in good agreement with the present calculations as well as the literature.[51,52] The calculated peaks at 1192 cm^{-1}, 1378 cm^{-1}, and 1581 cm^{-1} should be assigned to BH_3 scissor, NH_3 umbrella, and NH_3 scissor vibrations, respectively. For the $AB(NH_3)_n$ complexes, $AB(NH_3)_3$ is taken as a model, and a similar Raman spectrum to that from the experiment can be obtained, as shown in Supporting Information, Figure S8. For the B−N stretches, a slight peak broadening (766 cm^{-1}) suggests energy level splitting of B−N stretch, which should be due to (1) the interaction between B−N in AB molecule and near-by coordinated -NH_3; (2) the liquefaction of $AB(NH_3)_3$, leading to the decrease of crystallization. As shown in Table 1, for the $AB(NH_3)_3$ complexes, there are two possible isomers $(AB(NH_3)_3(NH_3)_0$ and $AB(NH_3)_2(NH_3)_1)$ with the same energies, although they have slightly different vibrational frequencies for B−N stretching. The B−N stretching at 759 cm^{-1} for $AB(NH_3)_3(NH_3)_0$ is quite close to the experimental value (766 cm^{-1}). For the B−H stretches, little change can be found as compared to the neat AB. Namely, the -BH_3 group and its environment show no obvious change after ammonia absorption. For the N−H stretches, the calculations show that there are four types of vibrational modes: the lower two correspond to the weak symmetric and antisymmetric stretches of the -NH_3 group of AB molecules, and the higher two correspond to the symmetric and antisymmetric stretches of the NH_3 molecule interacting with AB. This agrees well with the experimental result where the peak that corresponds to the N−H stretches shows a shoulder located at 3224 cm^{-1} (Supporting Information, Figure S8).

CONCLUSION

In summary, our findings clearly indicate the interesting novel phenomenon that solid-state AB, which seems to have no coordination site to accept the electron lone pair in the N atom, is effective in NH_3 absorption at 0 °C under an ammonia atmosphere. The novel phenomena and properties displayed by the reversible ammonia absorption/desorption of AB, such as liquefaction of AB, and the increasing mole ratios of NH_3/AB that appear with increasing ammonia pressure, may be of value for some potential applications, for example, separation and purification technologies for AB, loading into multiple-pore materials, and pressure sensitive materials for ammonia storage. As the simplest amine adduct, NH_3 is not likely to induce the concerns about steric hindering, in which classical adduct formation can be impaired, so we believe that this report will provide a classical and ideal model of the reaction between amines and AB. Furthermore, it can be expected that NH_3 binding to NH_4BH_4 most likely happens if only the conducted experiments are well controlled.

ASSOCIATED CONTENT

Supporting Information. Experimental details, Figures S1−S8, and Table S1. This material is available free of charge via the Internet at http://pubs.acs.org.

AUTHOR INFORMATION

Corresponding Author

*E-mail: yuxuebin@fudan.edu.cn.

Author Contributions

§Liang Gao and Haocheng Fang contributed equally to this work

■ ACKNOWLEDGMENT

This work was financially supported by the National Natural Science Foundation of China (Grant 51071047), the National Major Basic Research Program of China (2011CB808505), the Program for New Century Excellent Talents in Universities (NCET-08-0135) and the Ph.D. Programs Foundation of Ministry of Education of China (20090071110053). The authors would like to thank Prof. Robert Crabtree for his constructive suggestions on this work.

■ REFERENCES

(1) Taylor, R. C.; Cluff, C. L. *Nature* **1958**, *182*, 390.
(2) Shore, S. G.; Parry, R. W. *J. Am. Chem. Soc.* **1955**, *77*, 6084.
(3) Wolf, G.; Baumann, J.; Baitalow, F.; Hoffmann, F. P. *Thermochim. Acta* **2000**, *343*, 19.
(4) Baitalow, F.; Baumann, J.; Wolf, G.; Jaenicke-Rossler, K.; Leitner, G. *Thermochim. Acta* **2002**, *391*, 159.
(5) Baumann, J.; Baitalow, E.; Wolf, G. *Thermochim. Acta* **2005**, *430*, 9.
(6) Hamilton, C. W.; Baker, R. T.; Staubitz, A.; Manners, I. *Chem. Soc. Rev.* **2009**, *38*, 279.
(7) Crabtree, R. H.; Siegbahn, P. E. M.; Eisenstein, O.; Rheingold, A. L. *Acc. Chem. Res.* **1996**, *29*, 348.
(8) Richardson, T. B.; deGala, S.; Crabtree, R. H.; Siegbahn, P. E. M. *J. Am. Chem. Soc.* **1995**, *117*, 12875.
(9) Klooster, W. T.; Koetzle, T. F.; Siegbahn, P. E. M.; Richardson, T. B.; Crabtree, R. H. *J. Am. Chem. Soc.* **1999**, *121*, 6337.
(10) Yang, X. H.; Zhao, L. L.; Fox, T.; Wang, Z. X.; Berke, H. *Angew. Chem., Int. Ed.* **2010**, *49*, 2058.
(11) Mo, Y. R.; Song, L. C.; Wu, W.; Zhang, Q. N. *J. Am. Chem. Soc.* **2004**, *126*, 3974.
(12) Staubitz, A.; Soto, A. P.; Manners, I. *Angew. Chem., Int. Ed.* **2008**, *47*, 6212.
(13) Burg, A. B. *J. Am. Chem. Soc.* **1947**, *69*, 747.
(14) Shore, S. G.; Boddeker, K. W. *Inorg. Chem.* **1964**, *3*, 914.
(15) Parry, R. W.; Shore, S. G. *J. Am. Chem. Soc.* **1958**, *80*, 15.
(16) Schultz, D. R.; Parry, R. W. *J. Am. Chem. Soc.* **1958**, *80*, 4.
(17) Shore, S. G.; Girardot, P. R.; Parry, R. W. *J. Am. Chem. Soc.* **1958**, *80*, 20.
(18) Shore, S. G.; Parry, R. W. *J. Am. Chem. Soc.* **1958**, *80*, 8.
(19) Shore, S. G.; Parry, R. W. *J. Am. Chem. Soc.* **1958**, *80*, 12.
(20) Meng, Y.; Zhou, Z. Y.; Duan, C. S.; Wang, B.; Zhon, Q. *J. Mol. Struct. THEOCHEM* **2005**, *713*, 135.
(21) Li, J. S.; Zhao, F.; Jing, F. Q. *J. Chem. Phys.* **2002**, *116*, 25.
(22) Thorne, L. R.; Suenram, R. D.; Lovas, F. J. *J. Chem. Phys.* **1983**, *78*, 167.
(23) Yang, S. Y.; Fleurat-Lessard, P.; Hristov, I.; Ziegler, T. *J. Phys. Chem. A* **2004**, *108*, 9461.
(24) Siegbahn, P. E. M.; Eisenstein, O.; Rheingold, A. L.; Koetzle, T. F. *Acc. Chem. Res.* **1996**, *29*, 348.
(25) Li, J.; Zhao, F.; Jing, F. *J. Chem. Phys.* **2002**, *116*, 25.
(26) Allis, D. G.; Kosmowski, M. E.; Hudson, B. S. *J. Am. Chem. Soc.* **2004**, *126*, 7756.
(27) Gilbert, T. M. *J. Phys. Chem. A* **2004**, *108*, 2550.
(28) Meng, Y.; Zhou, Z.; Duan, C.; Wang, B.; Zhong, Q. *THEOCHEM* **2005**, *713*, 135.
(29) Singh, P. C.; Naresh Patwari, G. *Chem. Phys. Lett.* **2006**, *419*, 265.
(30) Yang, Y.; Zhang, W. *THEOCHEM* **2007**, *814*, 113.
(31) Li, J.; Kathmann, S. M.; Schenter, G. K.; Gutowski, M. *J. Phys. Chem. C* **2007**, *111*, 3294.
(32) Miranda, C. R.; Ceder, G. *J. Chem. Phys.* **2007**, *126*, 184703.
(33) Stowe, A. C.; Shaw, W. J.; Linehan, J. C.; Schmid, B.; Autrey, T. *Phys. Chem. Chem. Phys.* **2007**, *9*, 1831.
(34) At 273K, the critical pressure for liquefied ammonia is 4.340 bar NH_3, so 4 bar was chosen as the maximum pressure in our reaction process to make sure that NH_3 is in gaseous phase.
(35) Schwabe, T.; Grimme, S. *Phys. Chem. Chem. Phys.* **2006**, *8*, 4398.
(36) Câmpian, M. V.; Clot, E.; Eisenstein, O.; Helmstedt, U.; Jasim, N.; Perutz, R. N.; Whitwood, A. C.; Williamson, D. *J. Am. Chem. Soc.* **2008**, *130*, 4375.
(37) Seal, P.; Chakrabarti, S. *J. Phys. Chem. A* **2009**, *113*, 1377.
(38) Dunning, T. H. *J. Chem. Phys.* **1989**, *90*, 1007.
(39) Tomasi, J.; Mennucci, B.; Cammi, R. *Chem. Rev.* **2005**, *105*, 2999.
(40) Marenich, A. V.; Cramer, C. J.; Truhlar, D. G. *J. Phys. Chem. B* **2009**, *113*, 6378.
(41) Quemerais, P.; Raimbault, J. L.; Fratini, S. *J. Phys. IV* **2002**, *12*, 227.
(42) Gutowska, A.; Li, L. Y.; Shin, Y. S.; Wang, C. M. M.; Li, X. H. S.; Linehan, J. C.; Smith, R. S.; Kay, B. D.; Schmid, B.; Shaw, W.; Gutowski, M.; Autrey, T. *Angew. Chem., Int. Ed.* **2005**, *44*, 3578.
(43) Li, Z. Y.; Zhu, G. S.; Lu, G. Q.; Qiu, S. L.; Yao, X. D. *J. Am. Chem. Soc.* **2010**, *132*, 1490.
(44) Bowden, M.; Heldebrant, D. J.; Karkamkar, A.; Proffen, T.; Schenter, G. K.; Autrey, T. *Chem. Commun.* **2010**, *46*, 8564.
(45) Xiong, Z. T.; Wu, G. T.; Chua, Y. S.; Hu, J. J.; He, T.; Xu, W. L.; Chen, P. *Energy Environ. Sci.* **2008**, *1*, 360.
(46) Daly, S. R.; Bellott, B. J.; Kim, D. Y.; Girolami, G. S. *J. Am. Chem. Soc.* **2010**, *132*, 7254.
(47) Foster, J. P.; Weinhold, F. *J. Am. Chem. Soc.* **1980**, *102*, 7211.
(48) Reed, A. E.; Curtiss, L. A.; Weinhold, F. *Chem. Rev.* **1988**, *88*, 899.
(49) Flacau, R.; Ratcliffe, C. I.; Desgreniers, S.; Yao, Y. S.; Klug, D. D.; Pallister, P.; Moudrakovski, I. L.; Ripmeester, J. A. *Chem. Commun.* **2010**, *46*, 9164.
(50) As for calculation of vibrational frequencies, it is incorrect to directly use a gas phase AB molecule model since, in solid phase AB, the interaction between molecules cannot be neglected and have a severe impact on the mode of vibration. However, the geometry and frequencies of period AB solid using an accurate method is not practical for the limit of calculation method. From Supporting Information, Figure S3, the AB molecule can be regarded as the connection between NH_3 with a little positive charge and -BH_3 with a little negative charge, the structure of solid AB can be simply represented as Supporting Information, Figure S9 considering the similar polarity environments.
(51) Kang, X. D.; Ma, L. P.; Fang, Z. Z.; Gao, L. L.; Luo, J. H.; Wang, S. C.; Wang, P. *Phys. Chem. Chem. Phys.* **2009**, *11*, 2507.
(52) Hess, N. J.; Bowden, M. E.; Parvanov, V. M.; Mundy, C.; Kathmann, S. M.; Schenter, G. K.; Autrey, T. *J. Chem. Phys.* **2008**, *128*, 034508.